Threshold Measurements at the Internal Experimental Facility COSY–11

S. Brauksiepe, D. Grzonka, J. Haidenbauer, C. Hanhart, K. Kilian, R. Maier, W. Oelert, D. Prasuhn, T. Sefzick, M. Wolke* [a], M. Jochmann, M. Köhler, P. Wüstner[b], A. Hardt[c], H. Dombrowski, A. Khoukaz, T. Lister, C. Quentmeier, R. Santo, G. Schepers[d], L. Jarczyk, A. Kozela, P. Moskal, J. Smyrski, M. Sokołowski, A. Strzałkowski[e], J. Balewski, A. Budzanowski[f], C. Goodman[g], U. Seddik[h],

[a]Institut für Kernphysik, Forschungszentrum Jülich — KFA, 52425 Jülich, Germany

[b]Zentrallabor für Elektronik, Forschungszentrum Jülich — KFA, 52425 Jülich, Germany

[c]Fachhochschule Jülich, 52428 Jülich, Germany

[d]Institut für Kernphysik, Westfälische Wilhelms–Universität, 48149 Münster, Germany

[e]Institute of Physics, Jagellonian University, 30059 Cracow, Poland

[f]Institute of Nuclear Physics, 31342 Cracow, Poland

[g]Indiana University Cyclotron Facility, Bloomington, IN 47408, United States

[h]NRC, Atomic Energy Authority, P.O. 13759, Cairo, Egypt

The experimental setup and detection technique of the COSY–11 installation, an internal experimental facility at the cooler synchrotron and storage ring COSY Jülich, are described. The detection system has been designed for meson production studies with full geometrical acceptance close to threshold. Preliminary results of first measurements are presented, emphasis is put on strangeness production in the reactions $pp \to ppK^+K^-$ and $p \to pK^+\Lambda$.

1. Introduction

Although of fundamental nature, the production of single mesons and mesonic states with and without strangeness in a mass range from the π^0 to the $\Phi\,(1020)$ meson offers a broad field of unsolved questions in medium energy physics. One access to study different reaction mechanisms is provided by the proton proton interaction, the most elementary hadronic system available at COSY Jülich.

In threshold experiments, due to vanishing relative momenta of the ejectiles, baryon–baryon, baryon–meson and, with at least two mesons being produced, meson–meson final

*corresponding author, e–mail m.wolke@kfa-juelich.de

state interaction (FSI) should be observable. Additionally, close to threshold the theoretical interpretation of data is simplified by only S–waves contributing in the final state, and, from the experimental point of view, centre of mass 4π acceptance is feasible with a relatively small detection system.

2. Experimental Setup

A hydrogen cluster target with densities up to $\gtrsim 2 \times 10^{14}$atoms/cm^3 [1] has been installed in front of a regular C–type dipole magnet at an internal target location of the cooler synchrotron COSY [2].

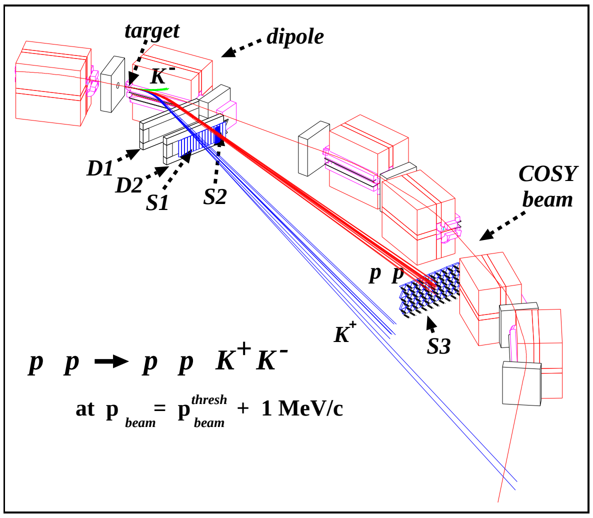

Figure 1. Three-dimensional display of the COSY–11 installation.

With the dipole being used as a magnetic spectrometer, positively charged ejectiles are separated from the circulating beam and diverted towards the centre of the storage ring after passing through a specially developed large exit foil of a vacuum chamber mounted inside the dipole gap. Including the knowledge of the dipole field, a measurement of the particles' direction by means of two drift chamber stacks (marked D1 and D2 in figure 1) allows the determination of their momentum vectors.

An arrangement of two scintillation hodoscopes is used to generate the trigger condition, i. e. to detect two protons in the exit channel in case of the predominantly studied $pp \rightarrow ppX$ reaction.

A time–of–flight measurement between the S1 scintillation counters and a large area scintillation wall (S3), spaced by a distance of 9.1 m, provides an initial value for the momentum reconstruction and allows a particle identification, supplemented by the specific energy loss information dE/dx from the scintillation counters.

Negatively charged mesons, bent towards the inside of the dipole gap, are detected by an array of silicon pad detectors mounted inside the gap.

A further silicon pad detector system is used to measure recoil protons originating from pp elastic scattering, which allows a normalization to obtain absolute cross sections and a calibration of the detector system. In case of the predominantly studied $pp \rightarrow ppX$ reaction resonances are identified by missing mass reconstructions from measured four–momenta of two outgoing protons. In addition, charged mesons either produced directly or from decays of X are detected with limited acceptance.

The geometrical acceptance of the COSY–11 detection system is limited by the narrow opening of the dipole gap with an internal height of 60 mm and decreases slowly with increasing excess energy above threshold, though close to threshold a 4π acceptance is realized. For a more detailed coverage of the COSY–11 detection system see ref. [3].

2.1. Beam Conditions

Simulations for the COSY–11 installation show that particularly an uncertainty in the point of interaction increases the width of reconstructed mass spectra. Thus, the target beam diameter has to be chosen rather small, but still large enough for a high luminosity measurement. However, demanding a high luminosity requires an optimum overlap of proton and target beam, the latter being reducible in size to a diameter of few mm.

The COSY beam dimensions at the internal target location are determined by the orbital shift for particles slightly differing from the ideal momentum, i. e. the dispersion, and the beta function, describing the envelope of the ideal beam. In co–operation with the COSY team, special "COSY–11" beam optics have been calculated, minimizing the dispersion and the beta function at the internal target location. Thus, by optimizing the focusing strength of quadrupoles, beam dimensions with a width in the order of the presently used cluster beam diameter of 9 mm are achieved [3].

3. Associated Strangeness Production in pp → ppK$^+$K$^-$

3.1. Motivation

While low lying pseudoscalar, vector and tensor mesons are described successfully as $q\overline{q}$ states on the basis of the quark model, the situation differs concerning scalar mesons.

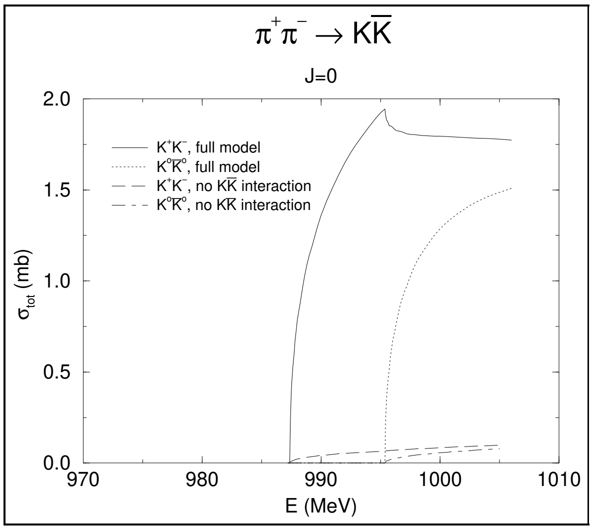

Figure 2. S–wave cross sections for the transitions $\pi^+\pi^- \to K^+K^-/K^0\overline{K^0}$ including (solid/dotted line) and neglecting (dashed/dashed dotted line) the strong $K\overline{K}$ interaction (taken from [7]).

A study of the reaction $pp \to ppK^+K^-$ is especially motivated by the discussion on the nature of the scalar resonances $f_0(975)$ and $a_0(980)$ in view of their affiliation to the scalar nonet.

A two–quark two–antiquark state within a nonet derived from colour–hyperfine interactions [4], a simple $q\overline{q}$ structure [5] and a $K\overline{K}$ molecule structure [6] have been suggested in case of the $f_0(975)$.

A recent analysis [7] in the framework of the Jülich meson exchange model for $\pi\pi$ and $\pi\eta$ scattering including the mass splitting between neutral and charged kaons concludes the f_0 to be a $K\overline{K}$ bound state: The threshold behaviour of the cross sections for $\pi\pi \to K\overline{K}$ shown in figure 2 is determined by the strong $K\overline{K}$ interaction resulting in a $K\overline{K}$ molecule identified with the $f_0(975)$.

In view of this, a measurement of the excitation function of K^+K^- production in the proton proton interaction in the region of the $K\overline{K}$ thresholds should reveal valuable information on the magnitude of the $K\overline{K}$ interaction and, thus, on the structure of scalar mesons in the $K\overline{K}$ threshold region.

3.2. Analysis Technique

A first step in singling out possible $pp \to ppK^+K^-$ events consists of demanding two identified protons in the exit channel. Particles are identified from the reconstructed three–momentum via the 'dipole spectrometer' and the drift chamber track reconstruction in combination with the time–of–flight measurement between the scintillation counters S1 and S3. Further analysis excludes all except for identified (pp) events.

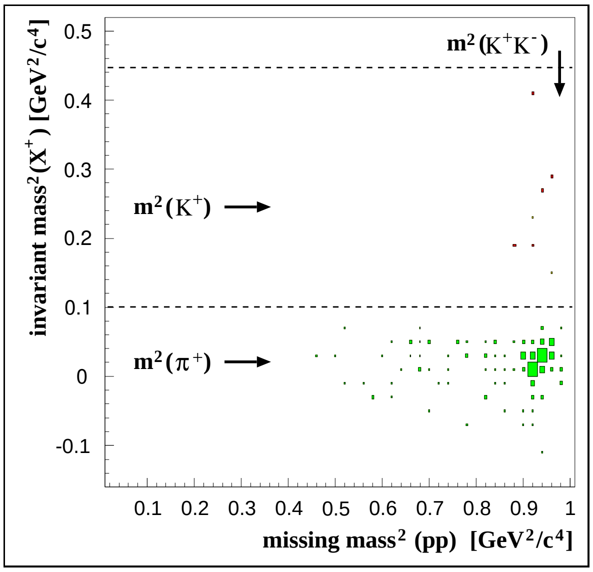

Figure 3. Squared invariant mass of particle A in $pp \to ppAB$ events versus the squared missing mass of the associated (pp) system.

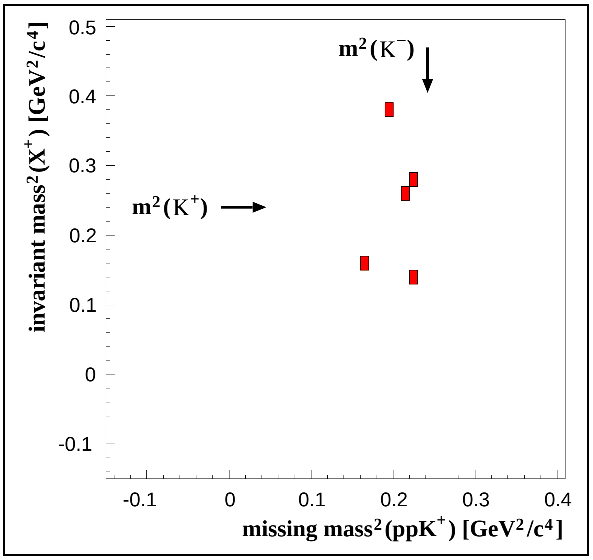

Figure 4. Squared missing mass of the (ppK^+) system corresponding to the mass of particle B versus squared invariant mass for particle A in $pp \to ppAB$ events.

Backtracking towards the nominal target position in view of the three–momentum reconstruction intrinsically provides the trajectory length between target and the S1 hodoscope. Thus, a target production time t_0 can be averaged out from both protons' path lengths and velocities.

Presently, data anlysis focuses on three track events, with the target production time allowing an indirect time–of–flight measurement between t_0 and "start" hodoscope S1, resulting in a mass identification for the third track not hitting the S3 scintillator, as it is expected for a positively charged kaon (see fig. 1). The invariant mass associated with the third detected track A from $pp \to ppAB$ events is plotted versus the missing mass in the (pp) system in figure 3. Signals from suspected positively charged kaons are well separated from the dominant pionic background. Figure 4 shows the missing mass in the suspected (ppK^+) system, i. e. the mass of the fourth ejectile B versus the reconstructed invariant K^+ mass, resulting in a total of 5 identified $pp \to ppK^+K^-$ events.

An efficiency $\eta = 0.19$ for the detection of three tracks, including the possible kaon decay, has been determined from Monte Carlo simulations. As the upper limit for the integrated luminosity is $L \times T \leq 180 \times 10^{33}\mathrm{cm}^{-2}$, a first preliminary estimate of the total cross section at 3.321 ± 0.003 GeV/c (corresponding to an excess energy of 6 MeV above threshold $\mathrm{p}_{beam}^{thresh} = 3.3016$ GeV/c) results in:

$$\sigma = \frac{N_{ppK^+K^-}}{\eta \times L \times T} \geq 150 \text{ pb} . \tag{1}$$

4. Λ–Hyperon Production via pp → pK$^+$Λ

4.1. Motivation

The associated strangeness production is an excellent tool to study reaction mechanisms and hadron dynamics in the nonperturbative region of strong interaction physics. The $s\bar{s}$ quark pair creation provides a clean signal on the reaction dynamics since there are no strange valence quarks in the proton proton initial state.

In nucleus–nucleus collisions, positively charged kaons are generally assumed to represent a lucid probe of the early phase, i. e. the high density and high temperature stage of the collision. The observed kaon yield should be sensitive to the nuclear equation of state applied for its theoretical description [8]. One major input of microscopic theoretical models consists of the elementary cross section.

Precise data on the production cross section especially in the threshold region are needed.

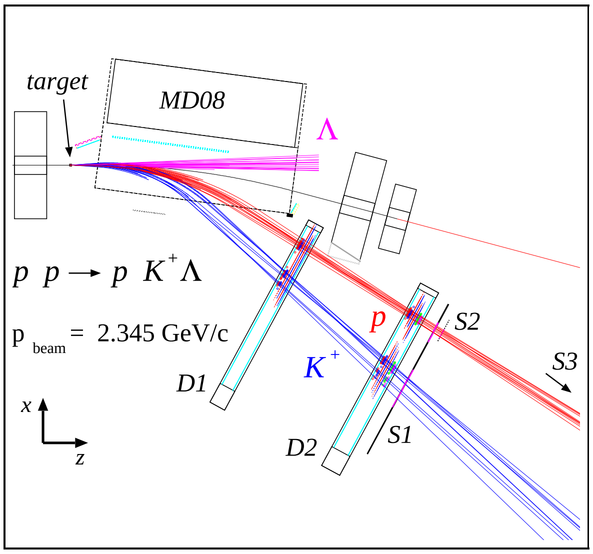

Figure 5. Experimental layout for the reaction $pp \to pK^+\Lambda$.

4.2. Method of Analysis

The experimental setup for the measurement of $pp \to pK^+\Lambda$ at a beam momentum of 2.345 GeV/c, i. e. at an excess energy of 2 MeV above threshold ($\mathrm{p}_{beam}^{thresh} =$ 2.339 GeV/c) is displayed in figure 5.

On the analogy of the technique described in case of the $pp \to ppK^+K^-$ reaction only events with one identified proton are considered for further analysis (fig. 6). Again, a mass identification for the second outgoing charged particle, as shown in figure 7 with the shaded area indicating the signal from detected kaons, is achieved via the indirect time–of–flight measurement.

For $pp \to pAX$ events, figure 8 shows an enhancement in the region of $(AX) = (K^+\Lambda)$, with the mass of X determined from energy and momentum conservation. The projection on the invariant mass of particle X with a cut on the K^+ mass (as indicated in fig. 8) results in a peak centered at 1.116 ± 0.002 GeV (FWHM ≈ 1 MeV), in very good agreement with the known Λ mass (fig. 9).

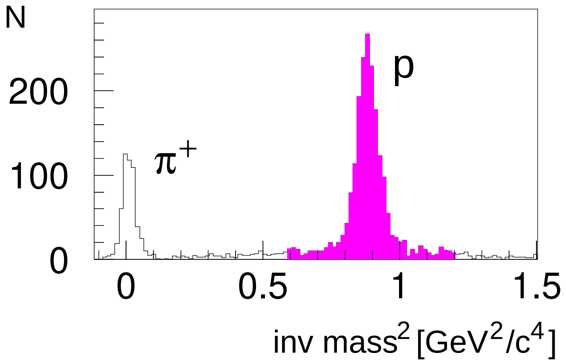

Figure 6. Squared invariant mass of particles passing the scintillators S1 and S3.

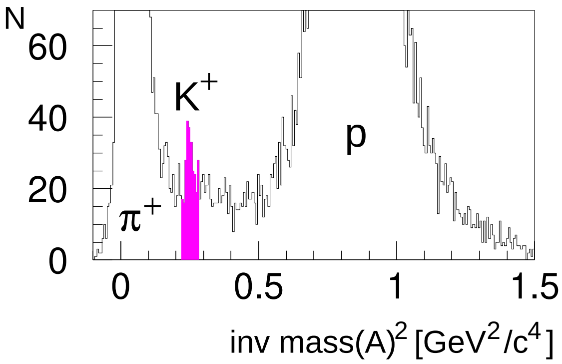

Figure 7. Squared invariant mass of the second charged particle A detected in coincidence with a proton.

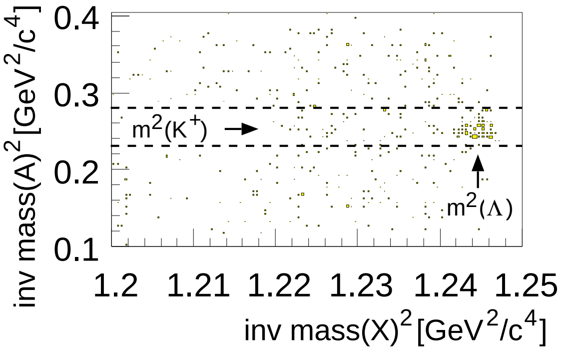

Figure 8. Squared invariant mass of charged particle A versus squared invariant mass of the unseen particle X for $pp \to pAX$ events.

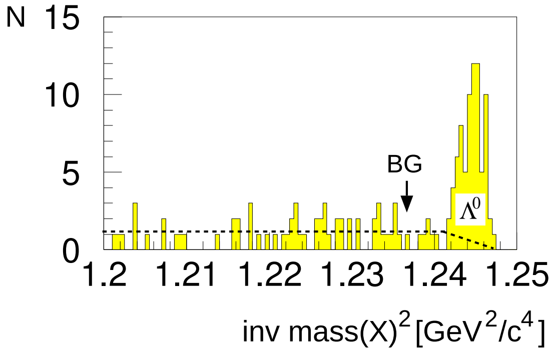

Figure 9. Squared invariant mass of X for $pp \to pK^+X$ events.

4.3. Results and Discussion

A total of 69 ± 7 $pp \to pK^+\Lambda$ events are identified with the error being due to background subtraction. The efficiency of the detection system for the reaction $pp \to pK^+\Lambda$ is determined from Monte Carlo simulations. This procedure has also been carried out for simultaneously measured pp elastic scattering used as a normalization, which bases in case of the $pK^+\Lambda$ reaction on differential cross sections for pp elastic scattering taken from [9, 10].

An integrated luminosity of $L \times T = (113 \pm 17) \times 10^{33}\mathrm{cm}^{-2}$ results in a total cross section for the $pK^+\Lambda$ reaction at a beam momentum $\mathrm{p}_{beam} = 2.345 \pm 0.002$ GeV/c of

$$\sigma = \frac{N_{pK^+\Lambda}}{\eta \times L \times T} = 8.2 \pm\ 1.8 \text{ nb}\ , \tag{2}$$

where $\eta = 0.075$ denotes the detection efficiency including the kaon decay and the error due to statistics, background subtraction, efficiency determination and luminosity.

We expect that the energy dependence of the $pp \to pK^+\Lambda$ cross section close to threshold is primarily determined by the (strong) interaction between the two baryons in the final state (as it turned out to be the case in the comparable reaction $pp \to pp\pi^0$ [11]). This is taken into account by Watson's model [13], where the production amplitude M is written as

$$\mid \mathrm{M} \mid^2 = \frac{\mid \mathrm{M}_0 \mid^2}{\mathrm{p}^2\,(1 + \cot\delta)}\ . \tag{3}$$

With the relative momentum p in the $(p\Lambda)$ system, the kaon momentum q in the corresponding three–body centre–of–mass system and substituting the effective range expansion for $\cot\delta$ the total cross section is determined as (for calculational details see [12])

$$\sigma = \frac{const}{\mid \vec{\mathrm{p}}_{beam} \mid} \int\limits_0^{\mathrm{q}_{max}} \frac{\mathrm{p} \cdot \mathrm{q}^2}{\mathrm{p}^2 + (-1/\hat{\mathrm{a}} + \hat{\mathrm{r}}\mathrm{p}^2/2)^2} d\mathrm{q}\ . \tag{4}$$

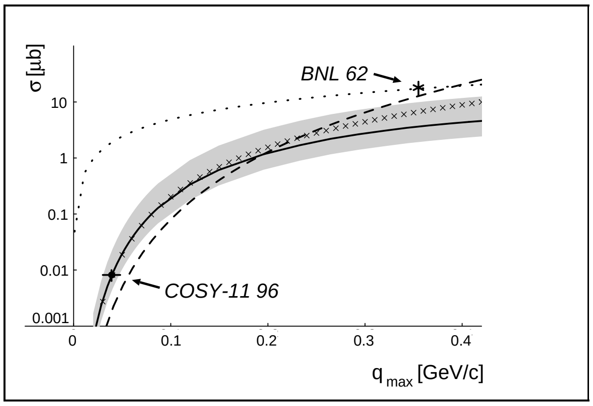

Figure 10. Total cross section for the reaction $pp \to pK^+\Lambda$. Theoretical descriptions from eqn. 4 (solid, the shaded area is due to the uncertainty of the beam momentum), impulse approximation calculations from [20] (crosses), and phenomenological parametrizations from [16] (dashed) and from [17,18] (dotted).

Figure 10 shows the predicted energy dependence of the total cross section close to threshold normalized to our data point. The shaded area results from the error on the beam momentum, effective range parameters $\hat{\mathrm{a}} = -1.6$ fm and $\hat{\mathrm{r}} = 2.3$ fm are taken from [14] and averaged for the possible S–wave singlet and triplet state of the $(p\Lambda)$ system. The underestimation of the data point taken from [15] is to be explained by at least P–waves contributing in this energy range. For comparison, results from the q^4 parametrization of Schürmann, Zwermann [16] and the linear approximation by Randrup, Ko [17,18] are included. These parametrizations often used in describing kaon yields in nucleus–nucleus collisions [19] do not seem to describe the threshold region of the elementary reaction.

In addition, results from an alternative theoretical approach for taking into account the baryon–baryon FSI [20] is shown by crosses in figure 10. The present data point is also reproduced within a factor of two by recent calculations in a one–boson exchange model [21].

Further investigations on $pp \to pK^+\Lambda$ are planned at the experimental facilities COSY–11 and COSY–TOF [22] at COSY Jülich.

Concluding Remark(s)

Results on $\pi^+\pi^-$ [23] and η as well as first encouraging data on η' production in the proton proton interaction have been left undisplayed within the framework of this presentation, but should at least be mentioned. This especially holds for a first study of a possible dibaryon resonance d' via $pp \to d'\pi^+ \to (pp\pi^-)\,\pi^+$ close to threshold [24], with data analysis being in progress.

In the near future, higher statistics data on η' production will be studied, data on K^+K^- are to be supplemented by additional measurements on the excitation function and an extension on the $pK^+\Lambda$ reaction is to be proposed.

The preliminary results presented here would not have been possible without the contributions of numerous people. We are thank the COSY team for preparing the proton beam for COSY–11.

REFERENCES

1. A. Khoukaz, STORI 96, Proc. of the Conf. (1996).
2. R. Maier et al. , EPAC 94, Proc. of the Conf. (1994) 165.
3. S. Brauksiepe et al. , Nucl. Instr. & Meth. A 376 (1996) 397.
4. R. Jaffe, Phys. Rev. D 15 (1977) 267.
5. D. Morgan, M. R. Pennington, Phys. Rev. D 48 (1993) 1185.
6. J. Weinstein, N. Isgur, Phys. Rev. D 41 (1990) 2236.
7. O. Krehl, R. Rapp, J. Speth, Report KFA–IKP(TH)–1996-09, KFA Jülich (1996) and references therein.
8. J. Aichelin, J. Jaenicke, in "Meson Production, Interaction and Decay", A. Magiera, W. Oelert, E. Grosse (eds.), World Scientific (1991).
9. K. A. Jenkins et al. , Phys. Rev. D 21 (1980) 2445.
10. D. T. Williams et al. , Nuovo Cim. A 8 (1972) 447.
11. H. O. Meyer et al. , Nucl. Phys. A 539 (1992) 633.
12. J. Balewski et al. , submitted for publication in Phys. Lett. B.
13. K. M. Watson, Phys. Rev. 88 (1952) 1163.
14. B. Holzenkamp et al. , Nucl. Phys. A 500 (1989) 485.
15. W. J. Fichinger et al. , Phys. Rev. 125 (1962) 2082.
16. B. Schürmann, W. Zwermann, Phys. Lett. B 183 (1987) 31.
17. J. Randrup, C. M. Ko, Nucl. Phys. A 343 (1980) 519.
18. J. Randrup, C. M. Ko, Nucl. Phys. A 411 (1983) 537.
19. G. Q. Li, C. M. Ko, Nucl. Phys. A 594 (1995) 439 and references therein.
20. G. Fäldt, C. Wilkin, Phys. Lett. B 382 (1996) 209.
21. A. Sibirtsev, Phys. Lett. B 359 (1995) 29.
22. K. Kilian, STORI 96, Proc. of the Conf. (1996).
23. A. Khoukaz, PhD Thesis (1996), Westfälische Wilhelms–Universität, Münster.
24. R. Bilger et al. , Prog. Part. Nucl. Phys. 36 (1996) 379.